microorganisms

MDPI

Article

The Disordered *C*-Terminus of the Chaperone DnaK Increases the Competitive Fitness of *Pseudomonas putida* and Facilitates the Toxicity of GraT

Sirli Rosendahl, Andres Ainelo and Rita Hõrak *

Department of Genetics, Institute of Molecular and Cell Biology, University of Tartu, Riia St 23, 51010 Tartu, Estonia; sirliluup@gmail.com (S.R.); andres.ainelo@gmail.com (A.A.)
* Correspondence: rita.horak@ut.ee

Abstract: Chaperone proteins are crucial for proper protein folding and quality control, especially when cells encounter stress caused by non-optimal temperatures. DnaK is one of such essential chaperones in bacteria. Although DnaK has been well characterized, the function of its intrinsically disordered *C*-terminus has remained enigmatic as the deletion of this region has been shown to either enhance or reduce its protein folding ability. We have shown previously that DnaK interacts with toxin GraT of the GraTA toxin-antitoxin system in *Pseudomonas putida*. Interestingly, the *C*-terminal truncation of DnaK was shown to alleviate GraT-caused growth defects. Here, we aim to clarify the importance of DnaK in GraT activity. We show that DnaK increases GraT toxicity, and particularly important is the negatively charged motif in the DnaK *C*-terminus. Given that GraT has an intrinsically disordered *N*-terminus, the assistance of DnaK is probably needed for re-modelling the toxin structure. We also demonstrate that the DnaK *C*-terminal negatively charged motif contributes to the competitive fitness of *P. putida* at both high and optimal growth temperatures. Thus, our data suggest that the disordered *C*-terminal end of DnaK enhances the chaperone functionality.

Keywords: toxin-antitoxin system; GraTA of HigBA family; DnaK chaperone; disordered domain; competitive fitness; *Pseudomonas putida*

Citation: Rosendahl, S.; Ainelo, A.; Hõrak, R. The Disordered *C*-Terminus of the Chaperone DnaK Increases the Competitive Fitness of *Pseudomonas putida* and Facilitates the Toxicity of GraT. *Microorganisms* **2021**, *9*, 375. https://doi.org/10.3390/microorganisms9020375

Academic Editors: Claudia Folli and Camilla Lazzi
Received: 14 January 2021
Accepted: 11 February 2021
Published: 13 February 2021

1. Introduction

Proper folding is of utmost importance for proteins to be able to complete their biological function. While most proteins have the intrinsic ability to obtain their correct structure, the folding process is essentially promoted by cellular chaperones. Chaperones not only assist the folding of newly synthesized proteins, but they also contribute to protein quality control by resolving and refolding misfolded protein aggregates or by delivering the aberrant proteins to cellular proteases for degradation [1,2]. Chaperones become particularly important under stress conditions, such as low or high temperature, heavy metals and oxidative stress, that promote protein misfolding and aggregation [3,4].

DnaK, with its co-chaperones DnaJ and GrpE, comprises an important component of the protein quality control chaperone network in bacteria [5,6]. DnaK is composed of an *N*-terminal nucleotide-binding domain (NBD), a *C*-terminal substrate-binding domain (SBD) and a short intrinsically disordered *C*-terminal tail with unclear function [7–9]. ATP binding and hydrolysis by DnaK NBD allosterically controls the binding of SBD to its substrates—short hydrophobic peptide segments that would normally be buried in the folded structure. This binding in turn enhances ATP hydrolysis by NBD [10,11]. DnaK facilitates the folding through repeated cycles of ATP-dependent binding and release of an unfolded protein [6]. While the *C*-terminal conserved disordered tail is not necessary for DnaK chaperone activity [12–14], it has been hypothesized to serve as an additional binding site for unfolded proteins [7]. However, the physiological importance of this possible auxiliary interaction between DnaK and its substrate proteins has remained

controversial, as it is unclear whether the truncation of the *C*-terminal tail enhances [8] or reduces the protein refolding activity of DnaK [7].

Interestingly, folding-assisting chaperones have been shown to be associated with the regulation of some toxin-antitoxin (TA) systems [15–17]. TA systems represent a family of two-gene loci that are widespread in mobile DNA, such as plasmids, transposons and phages, but also in bacterial chromosomes [18,19]. TA systems encode a toxic protein able to damage crucial biological processes or structures [20], and its antagonist that holds the toxin under strict control [21]. TA loci located in mobile elements serve as addiction modules that ensure stable maintenance of the mobile DNA [22,23]. This is conferred by the different stability of the toxin and the antitoxin. As antitoxins are usually less stable than toxins, the loss of mobile DNA results in the release of toxins, and thus growth suppression or death of the host [24,25]. Structural analysis on TA proteins has revealed that many antitoxins contain an unstructured region, which makes them susceptible to proteolysis [26,27]. Interestingly, some TA systems have recruited a chaperone gene to modulate the antitoxin stability. For example, the activity of a tripartite toxin-antitoxin-chaperone (TAC) module in *Mycobacterium tuberculosis* is controlled by a SecB-like chaperone [15,28]. The SecB homolog of the TAC operon contributes to toxin neutralization as the chaperone stabilizes the otherwise unstable antitoxin [15,16]. DnaK could be involved in the regulation of TA systems as well, as several *E. coli* antitoxins, i.e., DinJ, MazE, RelB and MqsA, belong to the DnaK interactome [5]. Intriguingly, in the *Pseudomonas putida* GraTA system, instead of the antitoxin, the toxin GraT was shown to interact with DnaK, and mutations in *dnaK* suppress GraT toxicity [17].

GraT is a member of the HigB family of toxins that belong to a RelE/ParE superfamily, which commonly encode ribosome-dependent RNases. In accordance with that, GraT is a ribosome-dependent mRNase toxin [29] which is neutralized by the antitoxin GraA [30]. The toxicity of GraT is highly temperature-dependent, being negligible at higher temperatures but gradually increasing at lower temperatures [30]. Atypical to an mRNase toxin, GraT causes a specific cold-dependent ribosome biogenesis defect characterized by the accumulation of ribosome precursors stalled at the late stages of their maturation [17]. The host bacterium tries to alleviate this GraT-caused defect by the upregulation of ribosome biogenesis factors, as evidenced by proteome analysis of the antitoxin deletion strain Δ*graA* [31]. GraT and GraA differ structurally from most other TA proteins as not the antitoxin but the toxin possesses an intrinsically disordered region [29]. While most antitoxins contain unstructured segments which make them susceptible to proteases [27,32], the antitoxin GraA is fully folded [29]. Consistently, GraA is an uncommonly stable protein, though its stability is decreased at the onset of stationary phase [33]. Unlike its closest homolog HigB and other TA toxins that are fully folded proteins [27,34], the toxin GraT contains an intrinsically disordered *N*-terminus [29]. This unstructured region of the toxin plays a dual role in GraTA regulation: it is required for GraT mRNase activity and toxicity, and it also acts as a derepressor of the *graTA* operon by preventing the binding of the GraTA complex to the operator [29]. Considering the partial disorder of GraT, it is highly interesting that GraT can interact with DnaK and that the *C*-terminal truncation of DnaK alleviates the GraT-caused ribosome biogenesis defect [17]. While the importance of the GraT-DnaK interaction remained unclear, two alternative hypotheses were proposed to explain the involvement of DnaK in the GraT-caused ribosome biogenesis defect [17]. The first hypothesis relies on the fact that DnaK participates in ribosome biogenesis [35,36], and poses that GraT directly attacks DnaK and inhibits its ability to assist ribosome maturation. The alternative hypothesis is that DnaK supports GraT toxicity, possibly by re-modelling the GraT structure.

Here, we aimed to clarify the role of DnaK in GraT toxicity. Our data suggest that DnaK enhances the GraT-caused phenotypes and that the most distal *C*-terminal end of DnaK is particularly important in the ability of DnaK to enhance GraT toxicity. We also addressed the question about the importance of the DnaK *C*-terminal disordered tail in *P. putida* fitness.

2. Materials and Methods

2.1. Bacterial Strains, Plasmids, and Growth Conditions

The bacterial strains and plasmids are listed in Table 1. *P. putida* strains used are derivatives of PaW85 [37], which is isogenic to the strain KT2440 [38,39]. Bacteria were grown in lysogeny broth (LB) medium. If selection was necessary, the growth medium was supplemented with ampicillin (100 μg mL^{-1}) or kanamycin (50 μg mL^{-1}) for *E. coli* and benzylpenicillin (1500 μg mL^{-1}), kanamycin (50 μg mL^{-1}) or streptomycin (200 μg mL^{-1}) for *P. putida*. Unless noted otherwise, *E. coli* was incubated at 37 °C and *P. putida* at 30 °C. Electrotransformation was carried out as described in [40].

Table 1. Bacterial strains and plasmids.

Strain or Plasmid	Genotype or Characteristic(s)	Source or Reference
E. coli strains		
DH5α λ*pir*	λ*pir* lysogen of DH5α	[41]
BL21(DE3)	*hsdS gal* (λcI *ts*857 *ind-1 S*am7 *nin-5 lacUV5*-T7 gene *1*)	[42]
P. putida strains		
PaW85	Wild-type, isogenic to KT2440	[37]
Δ*graA*	PaW85 Δ*graA*	[30]
tac-*dnaK*	PaW85 with *lacI*^{q}-P_{tac}-*dnaK* expression cassette in *glmS* locus (Sm^r)	This study
Δ*graA* tac-*dnaK*	Δ*graA* with *lacI*^{q}-P_{tac}-*dnaK* expression cassette in *glmS* locus (Sm^r)	This study
Δ*graA dnaK*$_{Δ41}$	Δ*graA* with 41 *C*-terminal amino acids truncated from DnaK	[17]
dnaK$_{mut4}$	DnaK carries substitution mutations D629N, E631Q, E633Q and E634Q	This study
Δ*graA dnaK*$_{mut4}$	Δ*graA* with DnaK carrying mutations D629N, E631Q, E633Q and E634Q	This study
secB	PaW85 *secB*::Sm (Sm^r)	This study
dnaK$_{mut4}$ *secB*	*dnaK*$_{mut4}$ with *secB*::Sm (Sm^r)	This study
wtSm	PaW85 with miniTn7-ΩSm in *glmS* locus	[38]
wtKm	PaW85 with miniTn7-Km in *glmS* locus	[38]
dnaK$_{mut4}$Sm	*dnaK*$_{mut4}$ with miniTn7-ΩSm in *glmS* locus	This study
dnaK$_{mut4}$Km	*dnaK*$_{mut4}$ with miniTn7-Km in *glmS* locus	This study
Plasmids		
pUCNot-lacItac	pUC18Not with *lacI*^{q}-P_{tac} cassette (Amp^r)	This study
pUCNotlacItac-dnaK	pUC18Not with *lacI*^{q}-P_{tac}-*dnaK* expression cassette (Amp^r)	This study
pBK-miniTn7-ΩSm	pUC19-based delivery plasmid for miniTn7-ΩSm (Amp^r Sm^r)	[43]
pminiTn7lacItac-dnaK	pBK-miniTn7-ΩSm with *lacI*^{q}-P_{tac}-*dnaK* expression cassette (Amp^r Sm^r)	This study
pBK-miniTn7-Km	pUC19-based delivery plasmid for miniTn7-Km (Amp^r Km^r)	[38]
pUXBF13	Plasmid coding for the Tn7 transposition proteins (Amp^r *mob*$^+$)	[44]
pEMG	Suicide plasmid containing *lacZ*α with two flanking I-SceI sites (Km^r)	[41]
pSW(I-SceI)	Plasmid for I-SceI expression (Ap^r)	[45]
pEMG-dnaK$_{mut4}$	pEMG with a PCR-designed 1040 bp XbaI-KpnI insert containing substitution mutations D629N, E631Q, E633Q and E634Q in the DnaK *C*-terminus	This study
pET11c	Protein expression vector (Ap^r)	Lab collection
pET-hisDnaK	pET11c for expression of DnaK with *N*-terminal His_6 tag (Ap^r)	[17]
pET-hisDnaK$_{C57}$	pET11c for expression of His_6-DnaK$_{C57}$, 57 *C*-terminal amino acids of DnaK are fused with *N*-terminal His_6 tag (Ap^r)	This study
pET-graT$_{Δ1C}$	pET11c for expression of GraT$_{Δ1C}$ (Ap^r)	[17]
pET-Δ22graT	pET11c for expression of *N*-terminally truncated Δ22GraT (Ap^r)	[29]
pT25	Plasmid encoding the T25 fragment (1–224 amino acids) of *cyaA* (Km^r)	[46]
pT18	Plasmid encoding the T18 fragment (225–399 amino acids) of *cyaA* (Ap^r)	[46]
pT25-zip	Plasmid encoding the T25 fragment fused with leucine zipper (Km^r)	[46]
pT18-zip	Plasmid encoding the T18 fragment fused with leucine zipper (Ap^r)	[46]
pT25-graT	Plasmid encoding the T25 fragment fused with *graT* (Km^r)	This study
pT18-graA	Plasmid encoding the T18 fragment fused with *graA* (Ap^r)	This study
pT18-dnaK$_{C44}$	Plasmid encoding the T18 fragment fused with 44 *C*-terminal amino acids of DnaK (Ap^r)	This study
pKS-secB	pBluescript KS containing PCR-amplified *secB* (PP_5053) (Amp^r)	This study
pUTmini-Tn5Sm/Sp	Delivery plasmid for mini-Tn5Sm/Sp (Amp^r Sm^r)	[47]
pKS-secB::Sm	Central 280 bp region of *secB* in pKS-secB is replaced by Sm^r gene (Amp^r Sm^r)	This study
pGP704L	Delivery plasmid for homologous recombination (Amp^r)	[48]
p704L-secB::Sm	pGP704L with Acc65I-SacI fragment of secB::Sm from pKS-secB::Sm (Amp^r Sm^r)	This study
pRK2013	Helper plasmid for conjugal transfer of pGP704L	[49]
pAG032	Broad-host-range reporter plasmid carrying P*ibpfxs-cfp*, P*rpsJ-yfp* and Pm-*rfp* promoter/reporter pairs	[50]

2.2. Construction of Plasmids and Strains

Oligonucleotides used in PCR amplifications are listed in Table 2. For the creation of DnaK overexpression strains, the *lacI*^{q}-P_{tac}-*dnaK* expression cassette was constructed. The *dnaK* gene fragment was amplified from the *P. putida* PaW85 chromosome with primers DnaKBam and dnaJdel, cut with EcoRI and BamHI and cloned into EcoRI-BamHI-opened pUCNot-lacItac. The *lacI*^{q}-P_{tac}-*dnaK* cassette was subcloned as a NotI fragment into the miniTn7 delivery plasmid pBK-miniTn7-ΩSm. The obtained pminiTn7lacItac-dnaK was introduced into *P. putida* wild-type and Δ*graA* strains by co-electroporation together with the helper plasmid pUXBF13. The presence of the expression cassette in the *attTn7* site of the tac-*dnaK* and Δ*graA* tac-*dnaK* strains was verified by PCR.

Table 2. Oligonucleotides.

Name	Sequence (5′-3′) [a]	Use
DnaKBam	aaggatccaaagtagtcgctgctacc	construction of pUCNotlacItac-dnaK
dnaJdel	aatcacgcttggacataggt	construction of pUCNotlacItac-dnaK and pT18-dnaK$_{C44}$
dnaKKpn	ccggtaccattcacgtgctgcaagg	construction of pEMG-dnaK$_{mut4}$
dnaK-3E1D	tgtctttcacttGttGgaactGggcgtTaaccacgtcat	construction of pEMG-dnaK$_{mut4}$
K-3E	CagttcCaaCaagtgaaagacaacaacaag	construction of pEMG-dnaK$_{mut4}$
dnaJXba	atgcctgcaggtcgactctagatcgacacctgcatggccatact	construction of pEMG-dnaK$_{mut4}$
secBalg	ctgctcgagagcaagggcgt	construction of pKS-secB
secBlopp	ggctctagaacgggtttgccgggag	construction of pKS-secB
T25-graT	aaactgcagcgattcgaagctttagctgtgc	construction of pT25-graT
1586Bam	cgggatccgttcttgagcatgatgc	construction of pT25-graT
T18-graA	aaagtcgacgctcaagaacggtatgcgtc	construction of pT18-graA
1585Bam	atggatccgtttttcgatgtcagtc	construction of pT18-graA
T18-dnaKsaba	tctggtaccggttgcccagaagatgta	construction of pT18-dnaK$_{C44}$
his-dnaK(C57)	aatcatatgcatcaccaccaccatcacgacgccaaggttgaagagct	construction of pET-hisDnaK$_{C57}$
dnaKSmaBam	attggatccccgggattactgcttgttgttg	construction of pET-hisDnaK$_{C57}$
dnaKqkeskFw	gtgccgaagtcctgaagaaa	qRT-PCR
dnaKqkeskRev	ctggctgtcgttgaagtagg	qRT-PCR
rpoDqFw	gcaacagcagtctcgtatca	qRT-PCR
rpoDqRev	atgatgtcttccacctgttcc	qRT-PCR

[a] The sites of restriction enzymes used in cloning are underlined. The mutated nucleotides are in uppercase letters.

For replacing the genomic wild-type *dnaK* allele with the *dnaK*$_{mut4}$, site-directed mutagenesis of *dnaK* was performed. For that, the upstream and downstream regions of *dnaK* *C*-terminus to be mutated were amplified separately with primer pairs dnaKKpn/dnaK-3E1D and K-3E/dnaJXba, respectively. Two PCR products were joined into an approximately 1-kb fragment by overlap extension PCR using primer pair dnaKKpn/dnaJXba. The PCR fragment was digested with KpnI and XbaI and cloned into pEMG. The obtained pEMG-dnaK$_{mut4}$ plasmid was delivered into *P. putida* PaW85 or Δ*graA* by electroporation, and after 3 h of growth in LB medium the bacteria were plated onto LB agar supplemented with kanamycin. Kanamycin-resistant cointegrates were selected and electrotransformed with the I-SceI expression plasmid pSW(I-SceI). To resolve the cointegrate, the plasmid-encoded I-SceI was induced with 1.5 mM 3-methylbenzoate overnight. Kanamycin-sensitive colonies were selected and the deletions were verified with PCR. The plasmid pSW(I-SceI) was eliminated from the deletion strains by growing them overnight in LB medium without antibiotics.

For the construction of *secB* deficient strains, the *secB* gene was amplified from the *P. putida* PaW85 genome with primers secBalg and secBlopp and cloned into XhoI-XbaI-opened pBluescript KS. In the obtained pKS-secB plasmid, the central 280-bp Van91I-PstI sequence of *secB* was replaced with the Sm^{r} gene, and the resulting *secB*::Sm sequence was subcloned as a SacI-Acc65I fragment into pGP704L. The interrupted *secB* gene was inserted into the chromosome of *P. putida* PaW85 and the *dnaK*$_{mut4}$ strains by homologous recombination. Plasmid p704L/secB::Sm was conjugatively transferred from *E. coli* CC118 λ*pir* into *P. putida* using the helper plasmid pRK2013. The *secB* deficiency of the strain was verified by PCR analysis.

For the construction of $dnaK_{mut4}$Sm and $dnaK_{mut4}$Km strains, miniTn7 delivery plasmids pBK-miniTn7-ΩSm or pBK-miniTn7-Km, respectively, together with pUXBF13 helper plasmid were coelectroporated into $dnaK_{mut4}$. Streptomycin or kanamycin resistant bacteria were selected and the miniTn7 insertion to *glmS* locus was verified by PCR.

The plasmids for the Bacterial Two-Hybrid (BACTH) assay were constructed as follows. The *graT* gene was amplified with primer pair T25-graT/1586Bam, and the PCR product was cleaved with PstI and BamHI and inserted into corresponding sites in pT25 to yield plasmid pT25-graT. Plasmid pT18-graA was constructed by the amplification of *graA* gene using primer pair T18-graA/1585Bam and cloning of the SalI-BamHI-cleaved PCR product into pT18. For the construction of plasmid pT18-dnaK$_{C44}$, the end of *dnaK* gene was amplified by primers T18-dnaKsaba and dnaJdel and the KpnI-EcoRI-cleaved PCR product was cloned into corresponding sites in pT18.

In order to construct the protein expression plasmid pET-hisDnaK$_{C57}$ for the pull-down assay, the *C*-terminal 57 amino acids of DnaK were fused with *N*-terminal His$_6$ tag by PCR with the aid of oligonucleotides his-dnaK(C57) and dnaKSmaBam. The resulting PCR fragment was treated with NdeI and BamHI and inserted into the corresponding sites in the pET11c plasmid.

2.3. qRT-PCR

Total RNA for *dnaK* mRNA quantification was isolated from exponential-phase bacteria using the RNAzol® RT and BAN (4-bromoanisole) reagents (Molecular Research Center, Inc., Cincinnati, OH, USA). The qRT-PCR assay was performed on the Rotor-Gene Q system (QIAGEN, Hilden, Germany) using the SuperScript® III Platinum® SYBR® Green One-Step qRT-PCR Kit (Thermo Fisher Scientific, Waltham, MA, USA) according to the manufacturer's protocol, except with double primer concentrations. For each reaction, 1 ng of total RNA was used. The *dnaK* gene was amplified using primers dnaKqkeskFw and dnaKqkeskRev, and the *rpoD* gene was amplified using primers rpoDqFw and rpoDqRev. Raw data were analyzed with the Rotor-Gene Q software v. 2.02 (QIAGEN) and mRNA amounts were calculated using the LinRegPCR software v. 2013.0 [51]. Data from at least three independent qRT-PCR experiments performed on two independently extracted RNAs were averaged and normalized against *rpoD* levels.

2.4. Temperature and Stress Tolerance Assays

After the bacteria were grown overnight in 5 mL of LB medium, 10-fold serial dilutions of the cultures were spotted as 5 µL drops onto LB plates with or without added chemicals (specified in Results). Plates were incubated at indicated temperatures for 24 or 48 h.

2.5. Growth Curves

The optical density of overnight bacterial cultures at 580 nm was measured and the cells were diluted in fresh LB medium for OD_{580} to be 0.1. Aliquots of 100 µL were transferred into microtiter plate wells and the cells were grown with shaking at 750 rpm at 30 °C, 34 °C or 37 °C, and OD_{580} was measured every 30 min with a TECAN Sunrise™ microplate reader.

2.6. Pull-Down Assay

The assay was performed as described previously [17]. Briefly, *E. coli* BL21(DE3) cultures carrying the pET-hisDnaK, pET-hisDnaK$_{C57}$, pET-graT$_{\Delta 1C}$ or pET-Δ22graT plasmids were pre-grown overnight at 37 °C and diluted into 200 mL fresh LB medium to a starting OD_{580} of around 0.1. All bacteria were grown at 30 °C for 2 h, after which the cultures expressing GraT$_{\Delta 1C}$ and Δ22GraT were transferred to 25 °C, while those expressing the DnaK variants remained at 30 °C. Protein expression was induced by the addition of 0.5 mM IPTG (Isopropyl β-D-1-thiogalactopyranoside) at an OD_{580}~0.6. After ~5 h of induction, the cells were pelleted and stored at −20 °C. For protein binding and purification, two pellets containing the proteins of interest were resuspended (50 mM Tris

pH 8.5; 0.5 M NaCl; 10 mM imidazole), mixed together and sonicated. The lysate was cleared by centrifugation and filtered through a 0.22 µm filter before loading it onto a 1 mL HisTrap HP (Cytiva, Uppsala, Sweden) column equilibrated with buffer A (50 mM Tris pH 8.5; 0.5 M NaCl; 50 mM imidazole). Protein purification was performed by fast protein liquid chromatography (FPLC) using an Äkta Prime chromatography system (GE Healthcare Life Sciences). Proteins were eluted using a linear 50–600 mM imidazole gradient. Samples from elution fractions with peak absorbance at 280 nm were collected, denatured and separated on 10% Tricine-SDS-PAGE. In parallel with Coomassie staining, the same samples were subjected to Western blotting using anti-GraT mouse antisera and alkaline phosphatase-conjugated goat anti-mouse antibodies. The blots were developed using bromochloroindolyl phosphate/nitro blue tetrazolium chloride (BCIP/NBT).

2.7. Bacterial Two-Hybrid Assay (BACTH)

The adenylate cyclase deficient *E. coli* reporter strain BTH101 was co-electroporated with two recombinant plasmids encoding hybrid proteins in which the proteins of interest were fused with either T25 or T18, i.e., fragments of *Bordetella pertussis* adenylate cyclase [46]. β-galactosidase activity was measured from bacteria grown on LB solid medium supplemented with 1 mM IPTG.

2.8. Measurement of Heat Shock Response

P. putida carrying the reporter plasmid pAG032 was grown at 30 °C in glucose minimal medium until OD_{600}~0.5. Then, some cultures were shifted to either 34 °C or 38 °C and after two hours of the temperature shift the OD_{600} and fluorescence (excitation 433 nm; emission 475 nm) were measured in a TECAN Infinite M200 PRO microplate reader. Fluorescence values were normalized to the OD_{600}.

2.9. Competition Assay

P. putida wild-type and $dnaK_{mut4}$ strains that are marked with an antibiotic resistance gene (streptomycin or kanamycin) were grown overnight in 5 mL LB medium at 30 °C. The optical densities of the bacterial cultures at 580 nm were measured and mixtures containing equal amounts of wtSm and $dnaK_{mut4}$Km or wtKm and $dnaK_{mut4}$Sm cells were prepared. The 1:1 mixtures were diluted 10,000-fold (about 10^5 cells per ml) into fresh 5 mL of LB and grown at 30 °C or 34 °C. Cells were diluted into fresh LB medium every 2 days and CFU/mL was measured every 4 days.

3. Results

3.1. DnaK mRNA Levels Are Unaltered in the ΔgraA Strain

Our previous data suggest that the GraT-caused growth inhibition and ribosome biogenesis defect is somehow associated with the chaperone and ribosome assembly factor DnaK [17]. Interestingly, whole-cell proteome comparison revealed that DnaK levels tended to be decreased in the Δ*graA* strain compared to wild-type, although the change was not statistically significant [31]. Therefore, considering that GraT is a ribosome-dependent mRNase [29], we hypothesized that GraT may target DnaK mRNA and the decreased abundance of DnaK results in the ribosome biogenesis defect. To test this possibility, we measured the *dnaK* mRNA levels in the *P. putida* wild-type and the Δ*graA* strain grown at 25 °C, where the GraT induces remarkable growth retardation [30]. qRT-PCR analysis revealed no significant differences in *dnaK* mRNA abundances between the wild-type and Δ*graA* strains (Figure 1). This refutes the possibility of *dnaK* mRNA being a specific target of GraT, and thus that the ribosome biogenesis defect may stem from DnaK depletion.

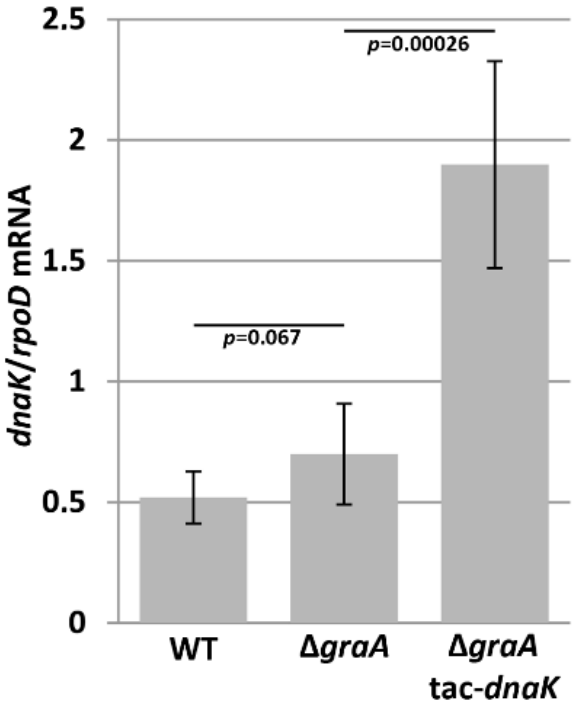

Figure 1. The *dnaK* mRNA levels are not affected by the GraT toxin. The relative abundance of the *dnaK*-specific mRNA in *P. putida* wild-type PaW85 (WT), Δ*graA* and Δ*graA* tac-*dnaK* strains were determined by qRT-PCR with *rpoD* as a reference gene. For induction of DnaK from the tac-*dnaK* cassette, 0.5 mM IPTG was used. Error bars represent the 95% confidence intervals from at least three independent experiments. *p* values of Student's *t*-test are indicated.

3.2. DnaK Enhances the Toxicity of GraT

GraT is a structurally exceptional protein among TA toxins as it contains an intrinsically disordered region, which is important for its activity [29]. Considering this and the finding that GraT can bind DnaK [17], we hypothesized that DnaK may assist GraT folding and enhance its toxicity. Notably, when searching for GraT suppressors, we identified only specific *dnaK* mutants where the transposon had disrupted the most distal *C*-terminal end of DnaK [17]. To further test whether DnaK is needed for GraT toxicity, we tried to construct the Δ*dnaK* and Δ*graA*Δ*dnaK* strains, but this turned out to be impossible, indicating that DnaK is essential for *P. putida*. We therefore used another approach and analyzed whether the chaperone overexpression could enhance the GraT effects. Thus, we introduced an inducible copy of *dnaK* into the Δ*graA* chromosome and evaluated the cold tolerance of bacteria. DnaK overexpression was verified by qRT-PCR at 25 °C, where 2.7-fold more *dnaK* mRNA was detected in the Δ*graA*-tac-*dnaK* strain compared to Δ*graA* (Figure 1). Growth assay on solid medium indicates that DnaK overexpression slightly increases the growth defect of Δ*graA* both at 30 °C and 25 °C (Figure 2A). As a control, we confirmed that the induction of DnaK in wild-type background has no effect on bacterial growth (Figure 2A). To further validate the model where DnaK enhances the GraT-caused growth inhibition, we also overexpressed DnaK in a Δ*graA* $dnaK_{\Delta 41}$ strain. This strain encodes for a truncated $DnaK_{\Delta 41}$ (lacking the 41 *C*-terminal amino acids) that largely suppresses GraT effects [17]; (Figure 2A). The overexpression of DnaK in the Δ*graA* $dnaK_{\Delta 41}$ strain overrides the alleviating effect of the $dnaK_{\Delta 41}$ allele and restores the cold-sensitive phenotype (Figure 2A). This result not only supports the positive role of DnaK in the GraT-caused growth defect, but also suggests that the *C*-terminal end of the chaperone plays a particularly important role in promoting GraT toxicity.

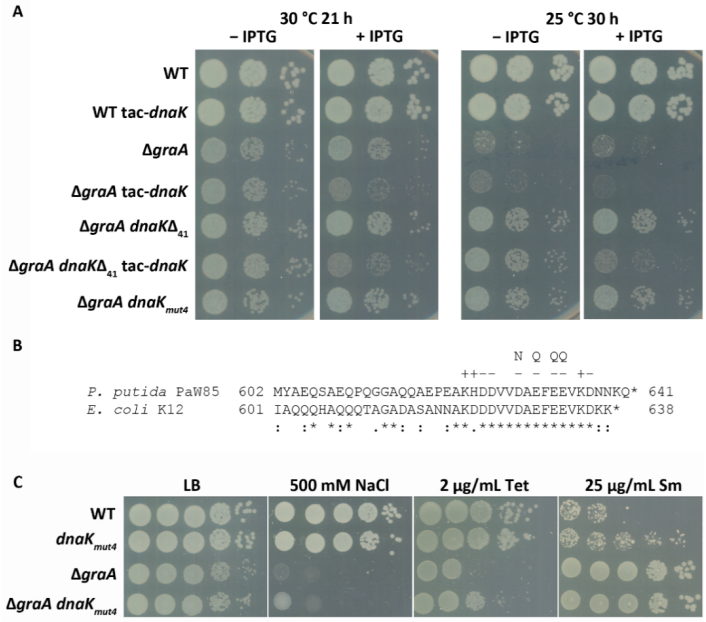

Figure 2. The conserved *C*-terminal domain of the DnaK is important for GraT toxicity. (**A**) Growth assay on a solid medium of the *P. putida* wild-type PaW85 (WT), Δ*graA* and their derivatives encoding the tac-*dnaK* overexpression cassette as well as Δ*graA* $dnaK_{\Delta 41}$ and Δ*graA* $dnaK_{mut4}$ strains encoding the DnaK with truncated or mutated *C*-terminus, respectively. Tenfold dilutions were spotted onto lysogeny broth (LB) medium and LB supplemented with 0.5 mM IPTG. Agar plates were incubated at 30 °C or 25 °C for indicated times. (**B**) Sequence alignment of *P. putida* PaW85 and *E. coli* K12 DnaK chaperone *C*-terminal ends. The charged amino acids in the conserved *C*-terminal motif are marked with "−" and "+". The four substitution mutations (D629N, E631Q, E633Q and E634Q) in the motif are indicated by N and Q. (**C**) Solid medium stress tolerance assays of *P. putida* wild-type, Δ*graA* and their $dnaK_{mut4}$ derivatives. Tenfold serial dilutions of the overnight cultures were spotted onto LB medium and on LB supplemented with NaCl, tetracycline or streptomycin. Final concentrations of the chemicals are indicated. Plates were incubated at 30 °C for 24 h (LB) or 48 h.

3.3. A Negatively Charged Motif in the DnaK C-Terminus Is Important for GraT Toxicity

The extreme *C*-terminus of DnaK is highly conserved (Figure 2B), and it has been proposed that this sequence acts as an auxiliary binding site for denatured proteins [7]. In order to test whether a specific feature of this conserved motif is important for supporting GraT toxicity, site-directed mutagenesis of DnaK was performed. Four negatively charged amino acids (D629, E631, E633 and E634) in the conserved end of DnaK were substituted with the respective polar residues Asn or Gln (Figure 2B). The wild-type *dnaK* gene in the Δ*graA* genome was replaced with the mutated $dnaK_{mut4}$ allele, and bacterial growth at 25 °C was analyzed. Data show that, similar to the *C*-terminus deletion, substitutions within the conserved end of DnaK significantly alleviate the growth defect of Δ*graA* (Figure 2A). Given that GraT has opposite effects on the stress tolerance of the Δ*graA* strain [30], we also analyzed whether the GraT-caused tolerance effects can be reversed or alleviated if the DnaK *C*-terminus is mutated. For that, we compared the stress tolerance of wild-type, $dnaK_{mut4}$, Δ*graA*, and Δ*graA* $dnaK_{mut4}$ strains on solid media supplemented with streptomycin, tetracycline or excess of NaCl. As expected, the tolerance of the Δ*graA* strain to tetracycline and NaCl was increased if this strain carried the $dnaK_{mut4}$ allele (Figure 2C). This is consistent with the finding that the *C*-terminal negatively charged motif contributes to the ability of DnaK to support GraT toxicity. Surprisingly, the tolerance of the Δ*graA* strain to streptomycin was not affected by the mutated *dnaK* gene (Figure 2C). However, we observed that the $dnaK_{mut4}$ strain displayed slightly higher streptomycin tolerance than the wild-type *P. putida* (Figure 2C). Thus, the mutated DnaK seems to affect streptomycin tolerance independent of its effects on GraT activity.

By using an in vitro pull-down assay, we have previously demonstrated that GraT binds to DnaK and also to its *C*-terminal truncation derivatives $DnaK_{\Delta 41}$ and $DnaK_{\Delta 66}$, which have retained their substrate binding domain [17]. However, as $DnaK_{\Delta 41}$ and $DnaK_{\Delta 66}$ are less efficient chaperones for GraT, the robust binding of the toxin to the SBD of DnaK seems to be insufficient to achieve full activation of GraT. To test whether the *C*-terminal domain of DnaK can give additional interactions with GraT, we performed an in vitro pull-down assay as well as used the bacterial two-hybrid (BACTH) system to detect protein binding in vivo.

For the pull-down assay, *E. coli* expressing His_6-$DnaK_{C57}$ (the *C*-terminal 57 amino acids of DnaK were fused with *N*-terminal His_6 tag) was mixed with cells expressing the nontoxic $GraT_{\Delta 1C}$ (lacks *C*-terminal histidine residue), and the mixed cell lysate was run through a Ni^{2+} affinity column. Analysis of column eluates on SDS-PAGE revealed purification of the His_6-$DnaK_{C57}$, but not the $GraT_{\Delta 1C}$ (Figure 3A). This result is consistent with previous data reporting that glutathione *S*-transferase fusion to the DnaK *C*-terminal end did not pull down any proteins from *E. coli* lysates [7]. Still, we tested whether the possible interaction between DnaK *C*-terminus and GraT can be detected in an in vivo BACTH assay [46]. For that, GraT was fused with the T25 fragment of the CyaA (plasmid pKT25-graT), and the 44 *C*-terminal amino acids of DnaK were fused with the T18 fragment of CyaA (plasmid pUT18C-$dnaK_{C44}$). As GraT binds its antitoxin GraA, GraA was also fused with the T18 fragment (plasmid pUT18C-graA) as a positive control. As expected, the co-expression of T25-graT and T18-graA fusions in *E. coli* BTH101 resulted in the activation of the *lacZ* reporter (Figure 3B). However, no reporter activity exceeding the negative control was detected when T25-graT was co-expressed with T18-$dnaK_{C44}$ fusion (Figure 3B). Thus, neither pull-down nor BACTH assays give evidence of a stable interaction between GraT and the *C*-terminus of DnaK.

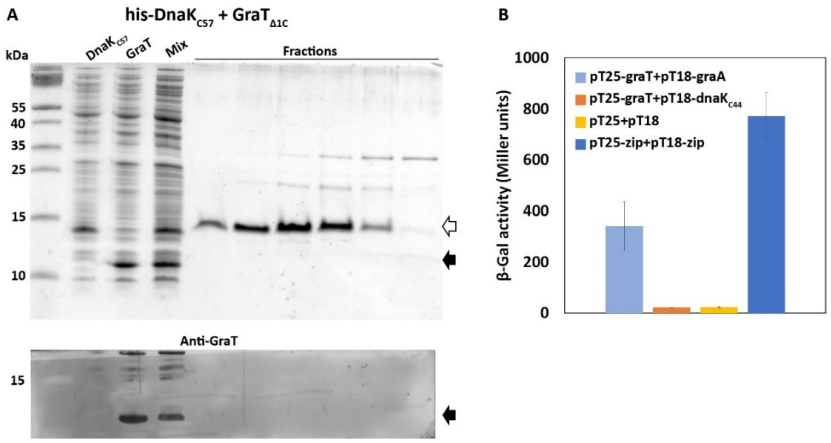

Figure 3. Stable interaction between GraT and *C*-terminal domain of DnaK could be detected neither in vitro nor in vivo. (**A**) An in vitro pull-down assay with His_6-$DnaK_{C57}$ as a bait protein for $GraT_{\Delta 1C}$. The cell lysate (Mix) prepared by mixing two *E. coli* cultures overexpressing either His_6-$DnaK_{C57}$ or $GraT_{\Delta 1C}$ was loaded onto Ni^{2+} affinity column and column elution fractions were analyzed on Coomassie-stained SDS-PAGE gel. Lower panel represents the Western blot analysis of an identical gel with anti-GraT antibodies. His_6-$DnaK_{C57}$ and $GraT_{\Delta 1C}$ are indicated by the empty and solid arrows, respectively. (**B**) An in vivo bacterial two-hybrid assay for analyzing the functional complementation between T25 and T18 fragments of *Bordetella pertussis* CyaA. β-galactosidase activities were measured in *E. coli* BTH101(Δ*cyaA*) co-transformed with two plasmids that encode proteins of interest (GraT, GraA, and 44 amino acid-long *C*-terminal end of DnaK) fused with T25 and T18. Plasmid pairs pT25+pT18 and pT25-zip+pT18-zip served as negative and positive controls, respectively. Bacteria were grown overnight at 37 °C on LB agar plates supplemented with 1 mM IPTG. The results are the average of four independent replicates and error bars represent the standard deviation.

3.4. The Disordered N-Terminus of GraT Is Not Essential for Binding to DnaK

GraT is a structurally unusual protein among TA-encoded toxins as it contains an intrinsically disordered *N*-terminus [29]. Given that DnaK interacts with unstructured proteins, we hypothesized that this disordered region of GraT could be the preferential binding site for DnaK. To test this possibility, we analyzed whether *N*-terminally truncated GraT lacking the first 22 residues (Δ22GraT) can co-purify with His_6-DnaK. The pull-down assay shows that Δ22GraT can interact with DnaK (Figure 4), indicating that the disordered *N*-terminus of the toxin is not essential for DnaK binding.

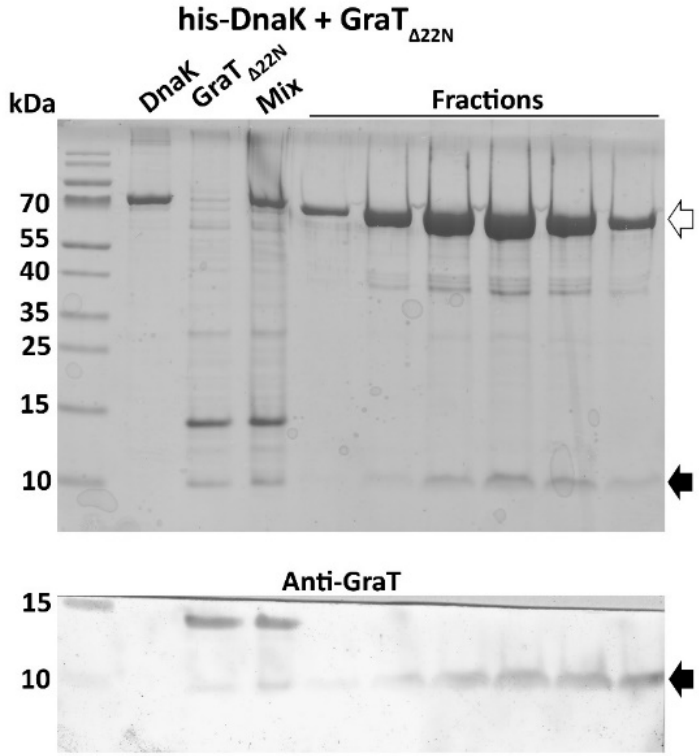

Figure 4. DnaK binds to *N*-terminally truncated GraT. His_6-DnaK pulls down the *N*-terminally truncated toxin $GraT_{\Delta 22N}$ from the cell lysate (Mix) prepared by mixing two *E. coli* cultures overexpressing either His_6-DnaK (DnaK) or $GraT_{\Delta 22N}$. Upper panel shows the Coomassie-stained lysates (DnaK, $GraT_{\Delta 22N}$, Mix) and elution fractions from the Ni^{2+} affinity column resolved by SDS-PAGE. Lower panel represents the Western blot analysis of an identical gel with anti-GraT antibodies. His_6-DnaK and $GraT_{\Delta 22N}$ are indicated by the empty and solid arrows, respectively.

3.5. The Negatively Charged Motif in the DnaK C-Terminus Contributes to Competitive Fitness of P. putida Not Only at High but Also at Optimal Temperature

The finding that the conserved *C*-terminal motif in DnaK plays an important role in supporting GraT toxicity prompted us to study other fitness effects that the DnaK *C*-terminus might have in *P. putida*. First, the growth of the wild-type and $dnaK_{mut4}$ strain was compared at different temperatures. Given that growth curves of two strains revealed no clear differences in any tested temperatures (Figure 5A), the substitution mutations in the DnaK *C*-terminus seem not to significantly influence the growth and thermotolerance of *P. putida*. To control whether temperatures higher than 30 °C can trigger the heat shock response, the activation of the σ^{32}-dependent P*ibpfxs* promoter was analyzed. Data show that transcription from P*ibpfxs* was upregulated already at 34 °C and even more at 38 °C (Supplementary Figure S1). Thus, despite the unaffected growth (Figure 5A), these temperatures do represent heat stress to *P. putida*.

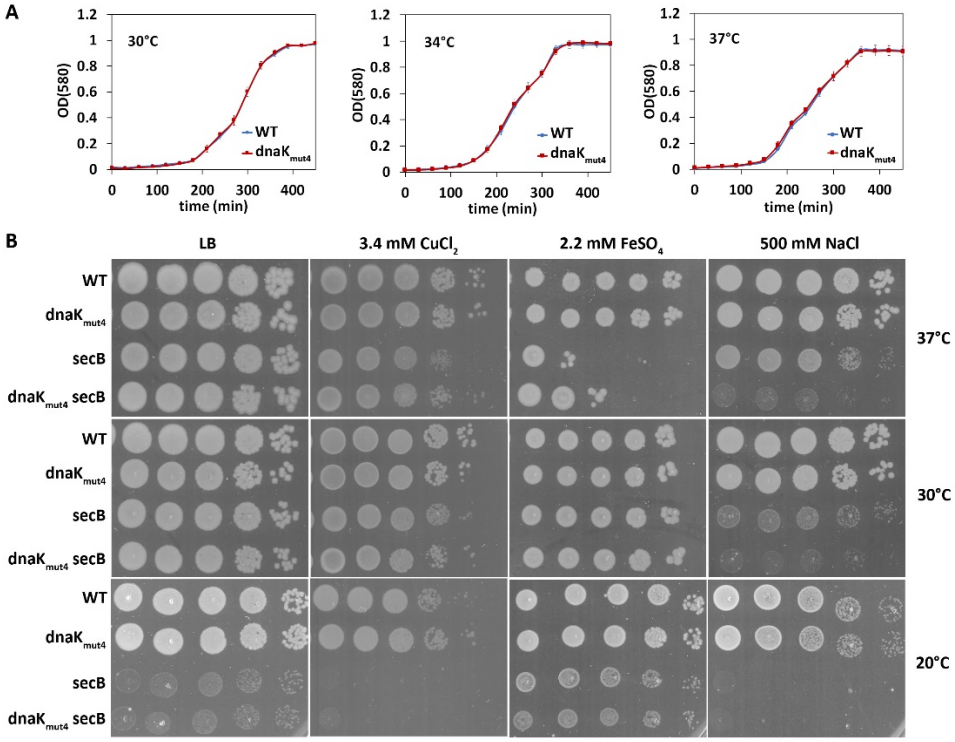

Figure 5. Mutation of the *C*-terminal conserved motif of DnaK results in no growth or heat tolerance defect in wild-type background, but affects the stress tolerance of *secB* deficient strain. (**A**) Growth curves of *P. putida* wild-type (WT) and $dnaK_{mut4}$ strains in LB medium at 30 °C, 34 °C and 37 °C. The strains were grown on microtiter plates. The results are the average of at least 15 replicates and error bars represent the standard deviation. (**B**) Solid medium stress tolerance assays of *P. putida* wild-type and $dnaK_{mut4}$ strains and their *secB* deficient derivatives. Tenfold serial dilutions of the overnight cultures were spotted onto LB medium and on LB supplemented with NaCl or metal salts. Final concentrations of the chemicals are indicated. Plates were incubated at indicated temperature for 24 h (LB and LB + 3.4 mM $CuCl_2$ at 37 °C and 30 °C) or 48 h.

Data in Figure 2C indicate that the streptomycin tolerance of the $dnaK_{mut4}$ strain is slightly increased. This prompted us to compare the wild-type and $dnaK_{mut4}$ strains under stress conditions that are known to boost protein misfolding and aggregation. Analysis of metal and sodium chloride tolerance revealed no clear difference between the wild-type and $dnaK_{mut4}$ strain at any tested temperature (Figure 5B). However, as defects in DnaK can be masked by other cellular chaperones [7,52], we also analyzed the temperature and stress tolerance of the $dnaK_{mut4}$ derivative deficient in chaperone SecB. Our data show that, similar to *E. coli* [52], deficiency in *secB* results in a cold-sensitive growth defect in *P. putida* (Figure 5B). Comparison of the $dnaK_{mut4}$ *secB* double mutant to the *secB* strain revealed that the double mutant was remarkably more sensitive to NaCl stress at 37 °C and 30 °C (Figure 5B). Contrary to that, however, the $dnaK_{mut4}$ *secB* strain was less sensitive to the excess of iron and also slightly to copper at 37 °C than the *secB* strain (Figure 5B). This indicates that the negatively charged motif in the DnaK *C*-terminus contributes to DnaK functionality, but its effects can be either positive or negative and seem to depend on the stress condition.

In order to test whether the DnaK *C*-terminal end can influence the competitive fitness of *P. putida*, a co-culture competition assay with mixed populations of wild-type and $dnaK_{mut4}$ strains was performed. Both strains were marked with kanamycin and streptomycin resistance genes. Growth curve analysis revealed that resistance genes had no effect on bacterial growth (Supplementary Figure S2). For the competition assay, 1:1 mixtures of wtKm:$dnaK_{mut4}$Sm as well as wtSm:$dnaK_{mut4}$Km were grown during 24 days in LB medium at 30 °C and 34 °C. Experiments at 37 °C were not possible as *P. putida* could not tolerate long-term cultivation at higher temperatures and bacteria died after the fourth day of co-cultivation. Over the 24 days of competition, bacteria pass about

144 generations, which is about ten times more than during growth curve experiments. The competition assay shows that the *C*-terminal conserved motif is important for DnaK functionality already at optimal temperature, as the *P. putida* wild-type strain displayed significant competitive advantage over the $dnaK_{mut4}$ strain at 30 °C (Figure 6A,B). Co-cultivation at 34 °C revealed a highly important role of the DnaK *C*-terminus for long-term thermotolerance of *P. putida* because the $dnaK_{mut4}$ strain was outcompeted from most mixed cultures of wild-type and $dnaK_{mut4}$ (Figure 6C,D). Interestingly, the out-competition dynamics of the $dnaK_{mut4}$ strain in separate mixed populations varied greatly at 34 °C, particularly after the 8th day of experiment, and there were some cultures where the ratio of $dnaK_{mut4}$ strain in the mix started to increase during the experiment (Figure 6C,D). The different fate of the $dnaK_{mut4}$ strain in parallel co-cultures suggests that the $dnaK_{mut4}$ strain experiences a high selection pressure, which may lead to regulatory or mutational changes.

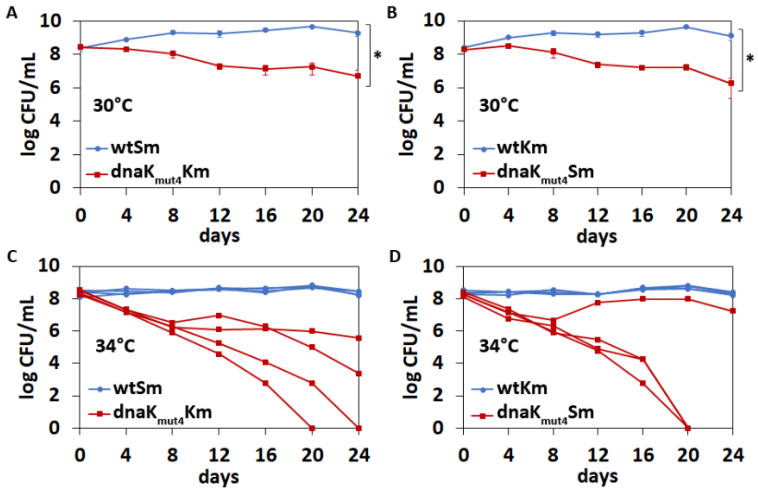

Figure 6. The negatively charged conserved motif in DnaK *C*-terminus is needed for competitive fitness of *P. putida*. Co-cultivation of *P. putida* wild-type and $dnaK_{mut4}$ strains that are marked with an antibiotic resistance gene (streptomycin or kanamycin). Panels A and C represent data for wtSm:$dnaK_{mut4}$Km cocultivation mixtures and panels B and D for wtKm:$dnaK_{mut4}$Sm mixtures. Bacteria were grown in LB medium at 30 °C or at 34 °C, diluted into a fresh LB medium every 2 days and CFU/mL was measured every 4 days. Means of four independent co-cultures with standard deviations are presented for experiments at 30 °C (**A**,**B**). For data obtained at 34 °C (**C**,**D**), each independent co-culture is graphed. Two-way ANOVA test was used to evaluate the difference between two strains over all time points (* $p < 10^{-16}$).

4. Discussion

TA systems are potentially deleterious to their host bacterium, and it is therefore not surprising that TA modules are tightly controlled. Most control over the toxin activity occurs through the regulation of antitoxin expression and stability. Besides the well-documented fact that the stability of antitoxins is affected by cellular proteases [32], there are also reports of protein folding chaperones being involved in correct folding and thus the stabilization of antitoxins [15,16]. Curiously, the current study demonstrates that toxin activity can also be positively affected by a cellular chaperone, as we show that DnaK facilitates the toxicity of GraT in the absence of its cognate antitoxin GraA. Another interesting finding of this study is that the enigmatic *C*-terminal disordered end of DnaK is important in shaping GraT toxicity. Furthermore, the conserved negatively charged motif in the DnaK *C*-terminus is necessary for *P. putida* competitive fitness.

The recruitment of a major host chaperone as a positive control factor of a toxin's activity is highly surprising, particularly when considering that GraT can fully arrest the host growth. The most reasonable explanation for chaperone addiction of GraT is that this toxin is intrinsically unable to fold correctly. This is supported by structural analysis of the

GraTA complex, which has revealed that the 22 amino acid-long *N*-terminus of GraT is disordered [29]. Interestingly, the disordered region of GraT has an important role in the regulation of the *graTA* operon, as this flexible segment hinders the binding of the GraTA complex to the operator and thus leads to the derepression of *graTA* transcription [29]. The switch between the GraA-mediated repression and the GraTA complex-mediated derepression of the *graTA* operon is highly relevant under conditions of high toxin:antitoxin ratio, as this allows de novo synthesis of antitoxin and thus prevents the accidental poisoning of host bacterium by the toxin GraT.

The unstructured *N*-terminus of GraT not only regulates *graTA* expression, but is also important for GraT toxicity and mRNase activity [29]. Structural data predict that the catalytically active site for mRNA degradation is located in the distal *C*-terminus of GraT, and that the *N*-terminus does not contribute to catalysis [29]. However, GraT cleaves mRNAs in a ribosome-dependent manner and should bind to the ribosome. Unfortunately, despite several efforts, we have not succeeded in isolating the ribosome-GraT complexes, indicating that the interaction between GraT and ribosome is weak and easily disrupted during ribosome purification. We propose that the *N*-terminal disordered segment of GraT could complicate the stable binding of the toxin to the ribosome, and this is probably the reason why the assistance of DnaK is required. Supporting evidence for the involvement of the toxin *N*-terminus in ribosome binding can be found from the structural analysis of the HigB of *P. vulgaris* [53]. *P. vulgaris* HigB is the closest homologue of GraT, and, except for the *N*-terminal disordered part, the structure of GraT resembles that of HigB [29,34]. Structural analysis of ribosome-HigB complexes showed that *P. vulgaris* HigB binds to the ribosomal A-site through two solvent-exposed basic regions [54], and, intriguingly, one of those interaction surfaces is located in the HigB *N*-terminus, i.e., just in the region which is unstructured in GraT. Substitutional mutagenesis of the HigB *N*-terminus suppressed its toxicity, which was considered to result from the decreased binding of HigB to the ribosome [54]. Analogously, the *N*-terminal truncation of GraT has been shown to eliminate the toxin mRNase activity and toxicity to the host [29]. We assume that, similar to HigB, the *N*-terminus of GraT participates in ribosome binding, but as it is intrinsically disordered, the assistance of DnaK is needed to fold GraT into the ribosome-binding-competent conformation.

An interesting feature of GraT toxin is that it causes cold-sensitive phenotypes. GraT greatly suppresses the growth of the antitoxin deletion strain Δ*graA* at 20 °C, but only slightly decreases the growth rate at 30 °C and has no effect on growth at 37 °C [30]. The involvement of the DnaK chaperone as a positive factor in GraT functionality suggests a plausible explanation for the temperature-sensitivity of GraT toxin. Higher temperatures cause the accumulation of misfolded and aggregated proteins and DnaK has a central role in their refolding and disaggregation [5]. It is therefore reasonable to assume that the interaction of DnaK with damaged proteins during heat stress titrates the chaperone away from binding to GraT. Hence, the deprivation of GraT of folding assistance at elevated temperatures results in non-toxic GraT. At lower temperatures, more DnaK is available for GraT binding and folding, and this results in more severe effects of GraT on cell growth. An alternative, but not mutually exclusive, explanation is that the spontaneous folding of GraT depends on temperature and occurs more correctly at lower temperatures.

Extensive studies have provided a detailed picture of the DnaK molecular mechanism that is regulated by the allosteric interactions between its nucleotide-binding domain and substrate binding domain [6]. However, much less is known about the biological role of the distal *C*-terminal disordered domain, which is not essential for DnaK chaperone activity [13,14]. To the best of our knowledge, the functional significance of the *C*-terminal domain of a bacterial DnaK is addressed in only two studies, which inconsistently propose that the extreme *C*-terminus may either reduce [8] or enhance the protein refolding activity of DnaK [7]. Our data are more consistent with the latter possibility because the *C*-terminal end positively impacts on DnaK's ability to enhance GraT toxicity. Mutagenesis of the *C*-terminal conserved negatively charged motif ^{625}DDVVDAEFEEVKD^{637} shows that this motif has a major role in the DnaK-mediated enhancement of GraT toxicity (Figure 2).

The other clear evidence for the positive effect of the *C*-terminal charged motif to DnaK functionality came from the competition assay, as replacing the charged ^{629}DAEFEE^{634} motif in the extreme end of DnaK with the sequence ^{629}NAQFQQ^{634} resulted in decreased competitive fitness of *P. putida* at optimal temperature, and even more at a higher temperature (Figure 6). We consider these results especially interesting because this is the first time when the mutagenesis of the DnaK *C*-terminal domain has resulted in a measurable deficiency of bacteria that have an otherwise wild-type genotype. In *E. coli*, DnaK *C*-terminal truncation has been shown to cause growth defects upon heat shock or SecB depletion [7]. However, these data were obtained with the *E. coli* derivative that has, in addition to *dnaK C*-terminal deletion, reduced levels of *dnaJ* expression as well as harbored a sigma S mutation that results in lower heat shock response [7,55]. Given that other cellular chaperones and heat shock proteins can compensate for the DnaK deficiency [7,56], such genetic background allowed the appearance of phenotypes caused by the *C*-terminal truncation of DnaK. Similar compensation of a *C*-terminal defect of DnaK seems to also occur in *P. putida*, as the growth and stress tolerance of the $dnaK_{mut4}$ strain were mostly equal to wild-type (the only exception was the slightly increased streptomycin tolerance of $dnaK_{mut4}$ compared to the wild-type; Figure 2C), and only when *secB* was disrupted did the defect of the $dnaK_{mut4}$ become evident in some stress conditions (Figure 5). However, the effect of the mutated $DnaK_{mut4}$ in the *secB* strain depended on the stress condition applied. Compared to the parent *secB* strain, the *secB*$dnaK_{mut4}$ derivative was less tolerant to NaCl stress but more tolerant to the excess of iron and copper (Figure 5). These data suggest that the *C*-terminal end of DnaK can have both positive and negative fitness consequences, at least when the chaperone SecB is deficient. Still, considering that the mutagenesis of the *C*-terminal motif in DnaK essentially decreased the long-term thermotolerance and competitive fitness in wild-type *secB* background, the disordered *C*-terminal domain confers a clear fitness advantage and therefore enhances rather than decreases the chaperone activity of DnaK.

It has been proposed that the unstructured *C*-terminus of DnaK comprises an auxiliary binding site for denatured client proteins, and that this additional transient binding would allow it to keep the client protein close to the chaperone after it is released from the canonical substrate-binding site [7]. This may support the repeated folding cycles of DnaK, and thus, facilitate the processing of misfolded proteins. Considering that many eukaryotic homologs of DnaK, the Hsp70s, also possess intrinsically disordered *C*-termini which contribute to substrate recognition and co-chaperone binding [57], the functioning of the *C*-terminal structural disorder in protein recognition seems to be evolutionarily conserved across the bacterial and eukaryotic chaperones.

Supplementary Materials: The following are available online at https://www.mdpi.com/2076-2607/9/2/375/s1, Figure S1: Heat shock response of *P. putida*, Figure S2: Growth curves of *P. putida* wild-type and $dnaK_{mut4}$ strains possessing streptomycin or kanamycin resistance genes.

Author Contributions: Conceptualization, R.H.; investigation and data analysis, S.R. and A.A.; visualization, S.R.; writing—original draft preparation, R.H., A.A. and S.R.; writing—review and editing, S.R., A.A. and R.H.; funding acquisition, project administration and supervision, R.H. All authors have read and agreed to the published version of the manuscript.

Funding: This research was funded by the Estonian Research Council, grant PUT1351, and by the University of Tartu ASTRA Project PER ASPERA, financed by the European Regional Development Fund.

Institutional Review Board Statement: Not applicable.

Informed Consent Statement: Not applicable.

Data Availability Statement: Data are contained within the article.

Conflicts of Interest: The authors declare no conflict of interest. The funders had no role in the design of the study; in the collection, analyses, or interpretation of data; in the writing of the manuscript, or in the decision to publish the results.

References

1. Balchin, D.; Hayer-Hartl, M.; Hartl, F.U. In vivo aspects of protein folding and quality control. *Science* **2016**, *353*. [CrossRef] [PubMed]
2. Finka, A.; Mattoo, R.U.; Goloubinoff, P. Experimental milestones in the discovery of molecular chaperones as polypeptide unfolding enzymes. *Annu. Rev. Biochem.* **2016**, *85*, 715–742. [CrossRef] [PubMed]
3. Bukau, B.; Walker, G.C. Cellular defects caused by deletion of the *Escherichia coli* DnaK gene indicate roles for heat shock protein in normal metabolism. *J. Bacteriol.* **1989**, *171*, 2337–2346. [CrossRef] [PubMed]
4. Winkler, J.; Seybert, A.; Konig, L.; Pruggnaller, S.; Haselmann, U.; Sourjik, V.; Weiss, M.; Frangakis, A.S.; Mogk, A.; Bukau, B. Quantitative and spatio-temporal features of protein aggregation in *Escherichia coli* and consequences on protein quality control and cellular ageing. *EMBO J.* **2010**, *29*, 910–923. [CrossRef]
5. Calloni, G.; Chen, T.; Schermann, S.M.; Chang, H.C.; Genevaux, P.; Agostini, F.; Tartaglia, G.G.; Hayer-Hartl, M.; Hartl, F.U. DnaK functions as a central hub in the *E. coli* chaperone network. *Cell Rep.* **2012**, *1*, 251–264. [CrossRef] [PubMed]
6. Mayer, M.P.; Gierasch, L.M. Recent advances in the structural and mechanistic aspects of hsp70 molecular chaperones. *J. Biol. Chem.* **2019**, *294*, 2085–2097. [CrossRef]
7. Smock, R.G.; Blackburn, M.E.; Gierasch, L.M. Conserved, disordered c terminus of DnaK enhances cellular survival upon stress and DnaK in vitro chaperone activity. *J. Biol. Chem.* **2011**, *286*, 31821–31829. [CrossRef]
8. Aponte, R.A.; Zimmermann, S.; Reinstein, J. Directed evolution of the DnaK chaperone: Mutations in the lid domain result in enhanced chaperone activity. *J. Mol. Biol.* **2010**, *399*, 154–167. [CrossRef]
9. Rosenzweig, R.; Nillegoda, N.B.; Mayer, M.P.; Bukau, B. The hsp70 chaperone network. *Nat. Rev. Mol. Cell Biol.* **2019**, *20*, 665–680. [CrossRef]
10. Kityk, R.; Vogel, M.; Schlecht, R.; Bukau, B.; Mayer, M.P. Pathways of allosteric regulation in hsp70 chaperones. *Nat. Commun.* **2015**, *6*, 8308. [CrossRef]
11. English, C.A.; Sherman, W.; Meng, W.; Gierasch, L.M. The hsp70 interdomain linker is a dynamic switch that enables allosteric communication between two structured domains. *J. Biol. Chem.* **2017**, *292*, 14765–14774. [CrossRef]
12. Buchberger, A.; Theyssen, H.; Schroder, H.; McCarty, J.S.; Virgallita, G.; Milkereit, P.; Reinstein, J.; Bukau, B. Nucleotide-induced conformational changes in the atpase and substrate binding domains of the DnaK chaperone provide evidence for interdomain communication. *J. Biol. Chem.* **1995**, *270*, 16903–16910. [CrossRef] [PubMed]
13. Moro, F.; Fernandez, V.; Muga, A. Interdomain interaction through helices a and b of DnaK peptide binding domain. *FEBS Lett.* **2003**, *533*, 119–123. [CrossRef]
14. Swain, J.F.; Schulz, E.G.; Gierasch, L.M. Direct comparison of a stable isolated hsp70 substrate-binding domain in the empty and substrate-bound states. *J. Biol. Chem.* **2006**, *281*, 1605–1611. [CrossRef] [PubMed]
15. Bordes, P.; Cirinesi, A.M.; Ummels, R.; Sala, A.; Sakr, S.; Bitter, W.; Genevaux, P. Secb-like chaperone controls a toxin-antitoxin stress-responsive system in *Mycobacterium tuberculosis*. *Proc. Natl. Acad. Sci. USA* **2011**, *108*, 8438–8443. [CrossRef] [PubMed]
16. Bordes, P.; Sala, A.J.; Ayala, S.; Texier, P.; Slama, N.; Cirinesi, A.M.; Guillet, V.; Mourey, L.; Genevaux, P. Chaperone addiction of toxin-antitoxin systems. *Nat. Commun.* **2016**, *7*, 13339. [CrossRef]
17. Ainelo, A.; Tamman, H.; Leppik, M.; Remme, J.; Hõrak, R. The toxin grat inhibits ribosome biogenesis. *Mol. Microbiol.* **2016**, *100*, 719–734. [CrossRef] [PubMed]
18. Makarova, K.S.; Wolf, Y.I.; Koonin, E.V. Comprehensive comparative-genomic analysis of type 2 toxin-antitoxin systems and related mobile stress response systems in prokaryotes. *Biol. Direct* **2009**, *4*, 19. [CrossRef]
19. Leplae, R.; Geeraerts, D.; Hallez, R.; Guglielmini, J.; Dreze, P.; Van Melderen, L. Diversity of bacterial type II toxin-antitoxin systems: A comprehensive search and functional analysis of novel families. *Nucleic Acids Res.* **2011**, *39*, 5513–5525. [CrossRef] [PubMed]
20. Schuster, C.F.; Bertram, R. Toxin-antitoxin systems are ubiquitous and versatile modulators of prokaryotic cell fate. *FEMS Microbiol. Lett.* **2013**, *340*, 73–85. [CrossRef]
21. Chan, W.T.; Espinosa, M.; Yeo, C.C. Keeping the wolves at bay: Antitoxins of prokaryotic type ii toxin-antitoxin systems. *Front. Mol. Biosci.* **2016**, *3*, 9. [CrossRef] [PubMed]
22. Fraikin, N.; Goormaghtigh, F.; Van Melderen, L. Type II toxin-antitoxin systems: Evolution and revolutions. *J. Bacteriol.* **2020**. [CrossRef] [PubMed]
23. Harms, A.; Brodersen, D.E.; Mitarai, N.; Gerdes, K. Toxins, targets, and triggers: An overview of toxin-antitoxin biology. *Mol. Cell* **2018**, *70*, 768–784. [CrossRef] [PubMed]
24. Jensen, R.B.; Gerdes, K. Programmed cell death in bacteria: Proteic plasmid stabilization systems. *Mol. Microbiol.* **1995**, *17*, 205–210. [CrossRef] [PubMed]
25. Van Melderen, L.; Bernard, P.; Couturier, M. Lon-dependent proteolysis of CcdA is the key control for activation of CcdB in plasmid-free segregant bacteria. *Mol. Microbiol.* **1994**, *11*, 1151–1157. [CrossRef] [PubMed]
26. Loris, R.; Marianovsky, I.; Lah, J.; Laeremans, T.; Engelberg-Kulka, H.; Glaser, G.; Muyldermans, S.; Wyns, L. Crystal structure of the intrinsically flexible addiction antidote maze. *J. Biol. Chem.* **2003**, *278*, 28252–28257. [CrossRef] [PubMed]
27. Loris, R.; Garcia-Pino, A. Disorder- and dynamics-based regulatory mechanisms in toxin-antitoxin modules. *Chem. Rev.* **2014**, *114*, 6933–6947. [CrossRef]

28. Sala, A.; Calderon, V.; Bordes, P.; Genevaux, P. Tac from *Mycobacterium tuberculosis*: A paradigm for stress-responsive toxin-antitoxin systems controlled by SecB-like chaperones. *Cell Stress Chaperones* **2013**, *18*, 126–135. [CrossRef]
29. Talavera, A.; Tamman, H.; Ainelo, A.; Konijnenberg, A.; Hadzi, S.; Sobott, F.; Garcia-Pino, A.; Hõrak, R.; Loris, R. A dual role in regulation and toxicity for the disordered n-terminus of the toxin grat. *Nat. Commun.* **2019**, *10*, 972. [CrossRef] [PubMed]
30. Tamman, H.; Ainelo, A.; Ainsaar, K.; Hõrak, R. A moderate toxin, GraT, modulates growth rate and stress tolerance of *Pseudomonas putida*. *J. Bacteriol.* **2014**, *196*, 157–169. [CrossRef] [PubMed]
31. Ainelo, A.; Porosk, R.; Kilk, K.; Rosendahl, S.; Remme, J.; Hõrak, R. *Pseudomonas putida* responds to the toxin GraT by inducing ribosome biogenesis factors and repressing tca cycle enzymes. *Toxins* **2019**, *11*, 103. [CrossRef]
32. Brzozowska, I.; Zielenkiewicz, U. Regulation of toxin-antitoxin systems by proteolysis. *Plasmid* **2013**, *70*, 33–41. [CrossRef] [PubMed]
33. Tamman, H.; Ainelo, A.; Tagel, M.; Hõrak, R. Stability of the GraA antitoxin depends on the growth phase, ATP level, and global regulator mext. *J. Bacteriol.* **2016**, *198*, 787–796. [CrossRef] [PubMed]
34. Schureck, M.A.; Maehigashi, T.; Miles, S.J.; Marquez, J.; Cho, S.E.; Erdman, R.; Dunham, C.M. Structure of the *Proteus vulgaris* higb-(higa)2-higb toxin-antitoxin complex. *J. Biol. Chem.* **2014**, *289*, 1060–1070. [CrossRef] [PubMed]
35. Maki, J.A.; Schnobrich, D.J.; Culver, G.M. The DnaK chaperone system facilitates 30s ribosomal subunit assembly. *Mol. Cell* **2002**, *10*, 129–138. [CrossRef]
36. Al Refaii, A.; Alix, J.H. Ribosome biogenesis is temperature-dependent and delayed in *Escherichia coli* lacking the chaperones DnaK or DnaJ. *Mol. Microbiol.* **2009**, *71*, 748–762. [CrossRef]
37. Bayley, S.A.; Duggleby, C.J.; Worsey, M.J.; Williams, P.A.; Hardy, K.G.; Broda, P. Two modes of loss of the Tol function from *Pseudomonas putida* mt-2. *Mol. Gen. Genet.* **1997**, *154*, 203–204. [CrossRef] [PubMed]
38. Rosendahl, S.; Tamman, H.; Brauer, A.; Remm, M.; Hõrak, R. Chromosomal toxin-antitoxin systems in *Pseudomonas putida* are rather selfish than beneficial. *Sci. Rep.* **2020**, *10*, 9230. [CrossRef] [PubMed]
39. Regenhardt, D.; Heuer, H.; Heim, S.; Fernandez, D.U.; Strömpl, C.; Moore, E.R.; Timmis, K.N. Pedigree and taxonomic credentials of *Pseudomonas putida* strain kt2440. *Environ. Microbiol.* **2002**, *4*, 912–915. [CrossRef] [PubMed]
40. Sharma, R.C.; Schimke, R.T. Preparation of electrocompetent *e. Coli* using salt-free growth medium. *Biotechniques* **1996**, *20*, 42–44. [CrossRef]
41. Martinez-Garcia, E.; de Lorenzo, V. Engineering multiple genomic deletions in gram-negative bacteria: Analysis of the multi-resistant antibiotic profile of *Pseudomonas putida* kt2440. *Environ. Microbiol.* **2011**, *13*, 2702–2716. [CrossRef] [PubMed]
42. Studier, F.W.; Moffatt, B.A. Use of bacteriophage t7 rna polymerase to direct selective high-level expression of cloned genes. *J. Mol. Biol.* **1986**, *189*, 113–130. [CrossRef]
43. Koch, B.; Jensen, L.E.; Nybroe, O. A panel of tn7-based vectors for insertion of the gfp marker gene or for delivery of cloned DNA into gram-negative bacteria at a neutral chromosomal site. *J. Microbiol. Methods* **2001**, *45*, 187–195. [CrossRef]
44. Bao, Y.; Lies, D.P.; Fu, H.; Roberts, G.P. An improved tn7-based system for the single-copy insertion of cloned genes into chromosomes of gram-negative bacteria. *Gene* **1991**, *109*, 167–168. [CrossRef]
45. Wong, S.M.; Mekalanos, J.J. Genetic footprinting with mariner-based transposition in *Pseudomonas aeruginosa*. *Proc. Natl. Acad. Sci. USA* **2000**, *97*, 10191–10196. [CrossRef] [PubMed]
46. Karimova, G.; Pidoux, J.; Ullmann, A.; Ladant, D. A bacterial two-hybrid system based on a reconstituted signal transduction pathway. *Proc. Natl. Acad. Sci. USA* **1998**, *95*, 5752–5756. [CrossRef]
47. De Lorenzo, V.; Herrero, M.; Jakubzik, U.; Timmis, K.N. Mini-tn5 transposon derivatives for insertion mutagenesis, promoter probing, and chromosomal insertion of cloned DNA in gram-negative eubacteria. *J. Bacteriol.* **1990**, *172*, 6568–6572. [CrossRef]
48. Pavel, H.; Forsman, M.; Shingler, V. An aromatic effector specificity mutant of the transcriptional regulator DmpR overcomes the growth constraints of *Pseudomonas* sp. strain CF600 on para-substituted methylphenols. *J. Bacteriol.* **1994**, *176*, 7550–7557. [CrossRef] [PubMed]
49. Figurski, D.H.; Helinski, D.R. Replication of an origin-containing derivative of plasmid rk2 dependent on a plasmid function provided in trans. *Proc. Natl. Acad. Sci. USA* **1979**, *76*, 1648–1652. [CrossRef]
50. Gawin, A.; Peebo, K.; Hans, S.; Ertesvag, H.; Irla, M.; Neubauer, P.; Brautaset, T. Construction and characterization of broad-host-range reporter plasmid suitable for on-line analysis of bacterial host responses related to recombinant protein production. *Microb. Cell. Fact.* **2019**, *18*, 80. [CrossRef]
51. Ruijter, J.M.; Ramakers, C.; Hoogaars, W.M.; Karlen, Y.; Bakker, O.; van den Hoff, M.J.; Moorman, A.F. Amplification efficiency: Linking baseline and bias in the analysis of quantitative PCR data. *Nucleic Acids Res.* **2009**, *37*, e45. [CrossRef] [PubMed]
52. Ullers, R.S.; Ang, D.; Schwager, F.; Georgopoulos, C.; Genevaux, P. Trigger factor can antagonize both SecB and DnaK/DnaJ chaperone functions in *Escherichia coli*. *Proc. Natl. Acad. Sci. USA* **2007**, *104*, 3101–3106. [CrossRef]
53. Schureck, M.A.; Dunkle, J.A.; Maehigashi, T.; Miles, S.J.; Dunham, C.M. Defining the mRNA recognition signature of a bacterial toxin protein. *Proc. Natl. Acad. Sci. USA* **2015**. [CrossRef] [PubMed]
54. Schureck, M.A.; Maehigashi, T.; Miles, S.J.; Marquez, J.; Dunham, C.M. mRNA bound to the 30s subunit is a higb toxin substrate. *RNA* **2016**, *22*, 1261–1270. [CrossRef] [PubMed]
55. Bukau, B.; Walker, G.C. Mutations altering heat shock specific subunit of RNA polymerase suppress major cellular defects of *E. coli* mutants lacking the DnaK chaperone. *EMBO J.* **1990**, *9*, 4027–4036. [CrossRef]

56. Ullers, R.S.; Luirink, J.; Harms, N.; Schwager, F.; Georgopoulos, C.; Genevaux, P. SecB is a bona fide generalized chaperone in *Escherichia coli*. *Proc. Natl. Acad. Sci. USA* **2004**, *101*, 7583–7588. [CrossRef]
57. Gong, W.; Hu, W.; Xu, L.; Wu, H.; Wu, S.; Zhang, H.; Wang, J.; Jones, G.W.; Perrett, S. The c-terminal GGAP motif of Hsp70 mediates substrate recognition and stress response in yeast. *J. Biol. Chem.* **2018**, *293*, 17663–17675. [CrossRef] [PubMed]